7. Deprez L, Weckhuysen S, Holmgren P et al. Clinical spectrum of early-onset epileptic encephalopathies associated with *STXBP1* mutations. Neurology 2010: 75: 1159–1165.
8. Hamdan FF, Piton A, Gauthier J et al. De novo *STXBP1* mutations in mental retardation and nonsyndromic epilepsy. Ann Neurol 2009: 65: 748–753.
9. Moretti P, Sahoo T, Hyland K et al. Cerebral folate deficiency with developmental delay, autism, and response to folinic acid. Neurology 2005: 64: 1088–1090.
10. Boone PM, Bacino CA, Shaw CA et al. Detection of clinically relevant exonic copy-number changes by array CGH. Hum Mutat 2010: 31: 1326–1342.
11. Engel J Jr. Report of the ILAE classification core group. Epilepsia 2006: 47: 1558–1568.
12. Lieber MR. The mechanism of double-strand DNA break repair by the nonhomologous DNA end-joining pathway. Annu Rev Biochem 2010: 79: 181–211.
13. Saitsu H, Tohyama J, Kumada T et al. Dominant-negative mutations in alpha-II spectrin cause West syndrome with severe cerebral hypomyelination, spastic quadriplegia, and developmental delay. Am J Hum Genet 2010: 86: 881–891.

Correspondence:
Dr Hirotomo Saitsu
Department of Human Genetics
Yokohama City University Graduate School of Medicine
3-9 Fukuura, Kanazawa-ku
Yokohama 236-0004
Japan
Tel.: +81 45 787 2606
Fax: +81 45 786 5219
e-mail: hsaitsu@yokohama-cu.ac.jp

REPORT

De Novo and Inherited Mutations in *COL4A2*, Encoding the Type IV Collagen α2 Chain Cause Porencephaly

Yuriko Yoneda,[1] Kazuhiro Haginoya,[2,3] Hiroshi Arai,[4] Shigeo Yamaoka,[5] Yoshinori Tsurusaki,[1] Hiroshi Doi,[1] Noriko Miyake,[1] Kenji Yokochi,[6] Hitoshi Osaka,[7] Mitsuhiro Kato,[8] Naomichi Matsumoto,[1] and Hirotomo Saitsu[1,*]

Porencephaly is a neurological disorder characterized by fluid-filled cysts or cavities in the brain that often cause hemiplegia. It has been suggested that porencephalic cavities result from focal cerebral degeneration involving hemorrhages. De novo or inherited heterozygous mutations in *COL4A1*, which encodes the type IV α1 collagen chain that is essential for structural integrity for vascular basement membranes, have been reported in individuals with porencephaly. Most mutations occurred at conserved Gly residues in the Gly-Xaa-Yaa repeats of the triple-helical domain, leading to alterations of the α1α1α2 heterotrimers. Here we report on two individuals with porencephaly caused by a heterozygous missense mutation in *COL4A2*, which encodes the type IV α2 collagen chain. Mutations c.3455G>A and c.3110G>A, one in each of the individuals, cause Gly residues in the Gly-Xaa-Yaa repeat to be substituted as p.Gly1152Asp and p.Gly1037Glu, respectively, probably resulting in alterations of the α1α1α2 heterotrimers. The c.3455G>A mutation was found in the proband's mother, who showed very mild monoparesis of the left upper extremity, and the maternal elder uncle, who had congenital hemiplegia. The maternal grandfather harboring the mutation is asymptomatic. The c.3110G>A mutation occurred de novo. Our study confirmed that abnormalities of the α1α1α2 heterotrimers of type IV collagen cause porencephaly and stresses the importance of screening for *COL4A2* as well as for *COL4A1*.

Porencephaly (MIM 175780) is a neurological disorder characterized by fluid-filled cysts or cavities in the brain.[1] It has been suggested that porencephalic cysts are caused by a disturbance of vascular supply leading to cerebral degeneration.[2,3] Porencephaly clinically causes hemiplegia (most often), tetraplegia, epilepsy, and intellectual disability.[4,5] Monozygous twinning, maternal cardiac arrest or abdominal trauma, a deficient protein C anticoagulant pathway, or cytomegalovirus infections are risk factors for sporadic porencephaly.[2,6] Recently, mutations in the gene encoding type IV collagen α1 chain (*COL4A1* [MIM 120130]) have been shown to cause familial porencephaly.[7] Since then, de novo and inherited *COL4A1* mutations have been reported,[8–10] confirming that *COL4A1* abnormalities are involved in both sporadic and familial porencephaly. Type IV collagens are basement membrane proteins that are expressed in all tissues including the vasculature. COL4A1 (α1 chain) and COL4A2 (α2 chain) are the most abundant type IV collagens, and form heterotrimers with 2:1 stoichiometry (α1α1α2).[11] A mouse model of the heterozygous *COL4A1* mutation (*Col4a1*$^{+/\Delta ex40}$) showed cerebral hemorrhage and porencephaly and displayed abnormalities of vascular basement membranes, such as uneven edges, inconsistent density, and highly variable thickness.[7] In addition, a dominant negative effect of the *Col4a1*$^{+/\Delta ex40}$ mutation was demonstrated on collagen IV α1α1α2 heterotrimer assembly and its secretion.[7] In humans, most mutations are substitutions of the conserved Gly residue in the Gly-Xaa-Yaa repeat of the triple-helical domain, and they have a dominant negative effect on heterotrimer formation.[11,12]

COL4A2 (MIM 120090), which encodes the type IV α2 collagen chain, is a possible candidate for porencephaly because its mutations may affect the α1α1α2 heterotrimer. Supporting this idea, osteogenesis imperfecta type I-IV (MIM 166200, 166210, 259420, and 166220), which is characterized by abnormal bone fragility and low bone mass, is caused by mutations in both *COL1A1* (MIM 120150) and *COL1A2* (MIM 120160) that may interfere with formation of the collagen I α1α1α2 heterotrimer.[13] Moreover, mice lines harboring *Col4a2* point mutations (*Col4a2*^{ENU415}, c.227G>T [p.Val31Phe]; *Col4a2*^{ENU4003} and *Col4a2*^{ENU4020}, c.2073G>A [p.Gly646Asp]) showed abnormalities of the lens, cornea, and vascular stability.[14] In the brains of the mutants, pseudocysts in the upper cortical plate, hemorrhages surrounding small blood vessels, and focal hemorrhagic necroses were observed, indicating that *Col4a2* mutations cause abnormalities of the cerebral vasculature similar to those caused by *Col4a1* mutations.[7,14] In this study, we screened for *COL4A2* mutations in 35 Japanese individuals with porencephaly. Substitutions of a Gly residue in the Gly-Xaa-Yaa repeat were identified in two individuals (individuals 1 and 2). Clinical information and peripheral blood samples were

[1]Department of Human Genetics, Yokohama City University Graduate School of Medicine, Fukuura 3-9, Kanazawa-ku, Yokohama 236-0004, Japan; [2]Department of Pediatrics, Tohoku University School of Medicine, Seiryo-machi 1-1, Aoba-ku, Sendai 980-8574, Japan; [3]Department of Pediatric Neurology, Takuto Rehabilitation Center for Children, Akiu-machi 20, Taihaku-ku, Sendai 982-0241, Japan; [4]Department of Pediatric Neurology, Morinomiya Hospital, Morinomiya2-1-88, Joto-ku, Osaka 536-0025, Japan; [5]Department of Neonatal Medicine and Pediatrics, Osaka Medical College, 2-7 Daigakumachi, Takatsuki, Osaka 569-8686, Japan; [6]Department of Pediatric Neurology, Seirei-Mikatahara General Hospital, 2-12-12 Sumiyoshi, Naka-ku, Hamamatsu 430-8558, Japan; [7]Division of Neurology, Clinical Research Institute, Kanagawa Children's Medical Center, 2-138-4 Mutsukawa, Minami-ku, Yokohama 232-8555, Japan; [8]Department of Pediatrics, Yamagata University School of Medicine, Iida-nishi 2-2-2, Yamagata 990-9585, Japan
*Correspondence: hsaitsu@yokohama-cu.ac.jp
DOI 10.1016/j.ajhg.2011.11.016.

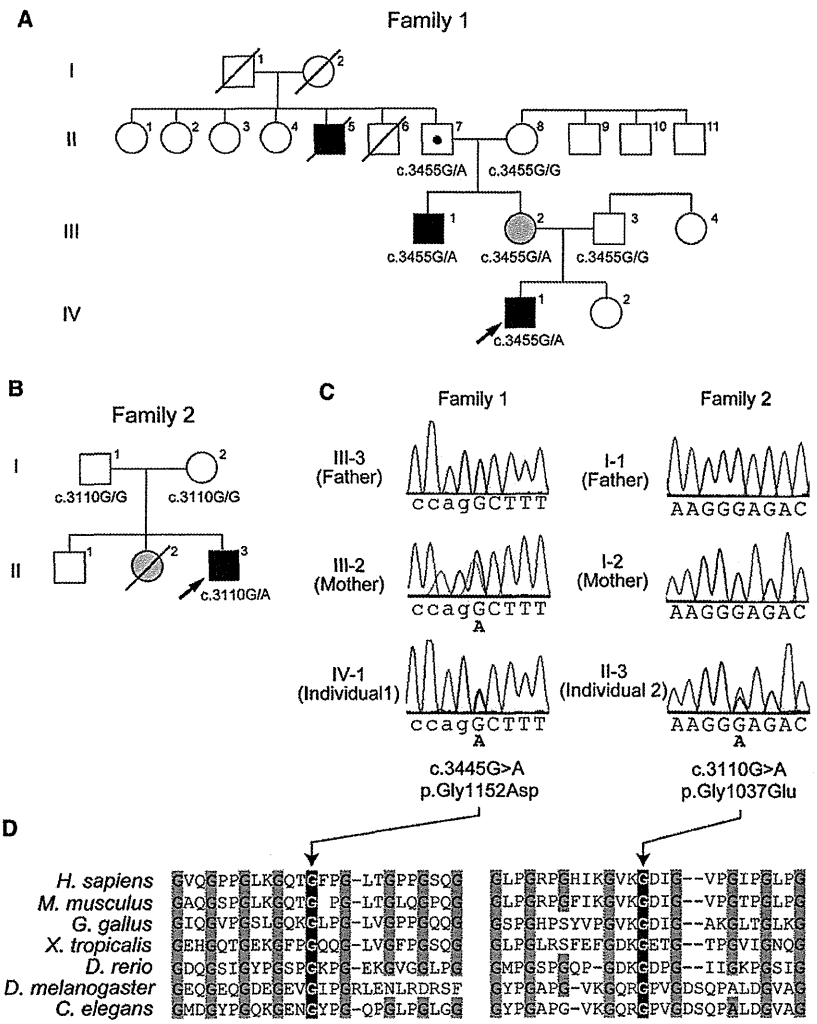

Figure 1. Pedigrees and *COL4A2* Mutations in Individuals 1 and 2

Pedigrees of family 1(A) and family 2 (B). The arrows indicate the probands (Individual 1 in family 1 and individual 2 in family 2). The segregation of the *COL4A2* mutations is shown. In family 1, the proband's mother (III-2) and maternal uncle (III-1) had mild monoparesis of the left upper extremity and congenital left hemiplegia and an assisted walk, respectively. The maternal grandfather (II-7) was healthy. The elder granduncle (II-5) was also afflicted by congenital hemiplegia and died in his 60s. (B) In family 2, the proband had a heterozygous mutation, but his parents did not have this mutation, indicating that the mutation occurred de novo. His elder sister (II-2) had intraventricular hemorrhage two days after birth but her DNA was unavailable.

(C) Electropherogram of family 1 (left) and family 2 (right). The intron and exon bases are in lower and upper cases, respectively. The c.3455G>A (p.Gly1152Asp) mutation in individual 1 was inherited from his mother. The c.3110G>A (p.Gly1037Glu) mutation in individual 2 occurred de novo.

(D) Multiple amino acid sequence alignments of COL4A2 proteins showing the evolutionarily conserved amino acids. The protein sequences obtained from the National Center for Biotechnology Information protein database are, NP_001837.2 (*Homo sapiens*), NP_034062.3 (*Mus musculus*), NP_001155862.1 (*Gallus gallus*), XP_002933063.1 (*Xenopus tropicalis*), XP_687811.5 (*Danio rerio*), AAB64082.1 (*Drosophila melanogaster*), and CAA80537.1 (*Caenorhabditis elegans*). The multiple sequence alignment was performed via the CLUSTALW website (see Web Resources). The positions of the conserved Gly residues in the Gly-X-Y repeats where the mutations occurred are highlighted with gray.

obtained from their family members after obtaining written informed consent. Experimental protocols were approved by the Institutional Review Board of Yokohama City University School of Medicine.

Individual 1 is 7 years old and a product of nonconsanguineous healthy parents (Figure 1A, arrow). There was no abdominal traumatism associated with the pregnancy and delivery in the mother. The individual was born at 36 weeks' gestation with a planned Caesarean section because, at 31 weeks' gestation, an antenatal ultrasound scan revealed an enlarged right lateral ventricle. Apgar scores were 9 at 1 min and 10 at 5 min. He weighed 2,900 g (+1.09 standard deviation [SD]) and had a head circumference of 32.5 cm (+0.05 SD). His early development was delayed with poor left hand use and abnormal leg movement. Brain magnetic resonance imaging (MRI) at 6 months showed an enlarged right lateral ventricle. Abrupt vomiting and nausea followed by motionless arrest developed at the 10 months. An electroencephalogram (EEG) showed focal spikes in the right frontal region, and carbamazepine treatment was initiated at the 12 months. Rehabilitation was started at 10 months. The individual started rolling at 12 months, crawling at 18 months, and walking alone at 3 years. He had spastic triplegia (diplegia and left hemiplegia) showing hemiplegic and diplegic gait with fluent speech and normal word comprehension. At the 5 years of age, he underwent orthopedic surgery for foot deformity due to spastic paresis. An EEG showed spikes in the right occipital to posterior temporal region and midcentral region. A brain MRI at age 6 showed an enlarged right lateral ventricle, reduced volume of the right frontal white matter, and atrophic right cerebral peduncle and body of corpus callosum (Figures 2A–2C). His intelligent quotient [IQ] score, evaluated at 6 years with Wechsler Intelligence Scale for Children-Third Edition (WISC-III), was 74 (his performance IQ was 69 and his verbal IQ was

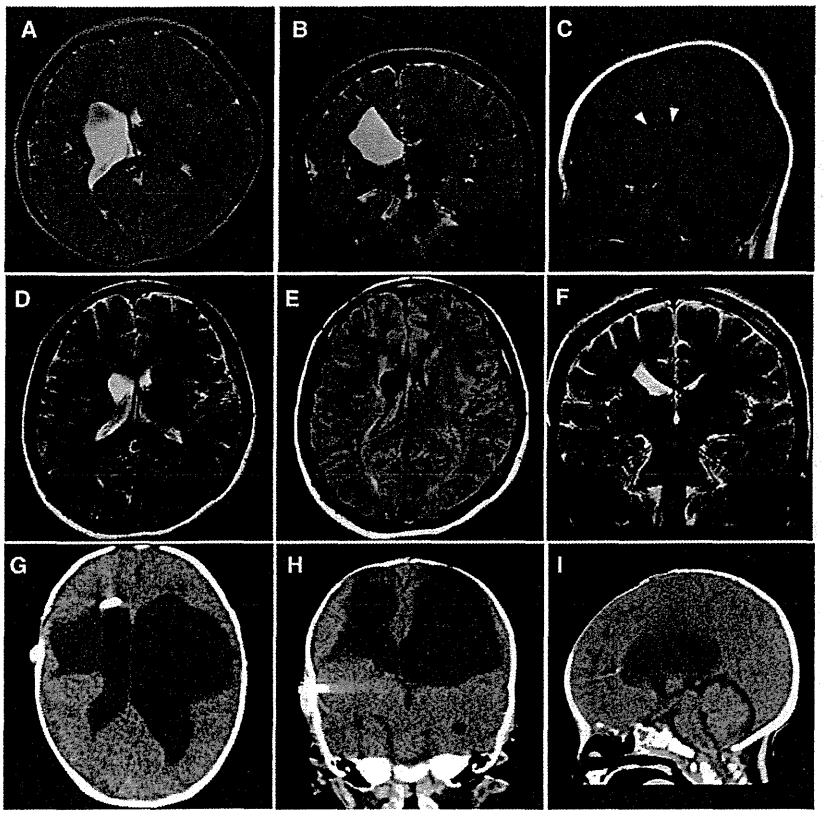

Figure 2. Brain Imaging in Individuals 1 and 2

(A–C) Brain MRIs of individual 1 at 6 years old; (A) T2-weighted axial image. (B) Coronal image. The images in (A) and (B) show an enlarged right lateral ventricle and a reduced volume of the right frontal white matter. (C) T1-weighted midline sagittal image showing atrophy of the body of the corpus callosum (arrowheads). The lesion responsible for the left leg paresis is not evident in these images.

(D–F) Brain MRIs of individual 1's mother at age 31. (D) T2-weighted axial and (F) coronal images show a mildly enlarged right lateral ventricle. (E) FLAIR axial image shows high signal intensity around the enlarged ventricular wall, which is consistent with mild porencephaly or periventricular venous infarction.

(G–I) CT images of individual 2 at 2 months of age. (G) Axial image. (H) Coronal image. (I) Sagittal image. The images in (G), (H), and (I) show an enlarged bilateral lateral ventricle and an extremely reduced volume of bilateral frontal white matter. The V-P shunt tube is also visible in the right lateral ventricle. The pontocerebellar structures seem to be normal.

82). The individual is now 7 years old and attending a local school. He can walk with ankle foot orthosis and hand assist. The epilepsy is well controlled with carbamazepine and clobazam. He does not show hematuria, muscular cramps, or ophthalmic abnormalities. His mother was born at term without asphyxia after an uneventful pregnancy. She had convulsions at the age of 18 months, and anticonvulsant was started under a diagnosis of focal epilepsy. Seizures were well controlled and treatment was discontinued at the age of 13. She first realized clumsiness of the left hand when she started learning piano and recorder at the age of 9. When she was a junior high school student, she felt severe headaches, and abnormal findings were pointed out in the brain MRI study (detailed information was unavailable). However, she did not undergo any more examinations because the headaches disappeared and did not recur. Neurological examination at 31 years revealed very mild monoparesis of the left upper extremity. She had neither spasticity nor exaggerated tendon reflexes. The grip power of her right and left hands was 25 and 15 kg, respectively. Mirror movement was observed on the right hand. The brain MRI revealed a mildly enlarged right lateral ventricle and high signal intensity around the enlarged ventricular wall on a Fluid Attenuated Inversion Recovery (FLAIR) image, which is consistent with mild porencephaly or periventricular venous infarction (Figures 2D–2F). MR angiography showed no aneurysms. Of note, his maternal elder uncle also showed congenital left hemiplegia with an assisted walk, and his maternal granduncle had also been afflicted by congenital hemiplegia, suggesting a genetic predisposition in the family (Figure 1A).

Individual 2 is 1 year and 4 months old and a product of nonconsanguineous healthy parents (Figure 1B, arrow). There was no abdominal traumatism associated with the pregnancy and delivery in the mother. He was born at 35 weeks' gestation. His birth weight was 1,694 g (−2.36 SD) and his head circumference was 29 cm (−1.77 SD). Mild asphyxia was observed, and he had Apgar scores of 3 at 1 min and 7 at 5 min. An ultrasound scan at 6 hr after birth revealed a parenchymal hemorrhage of the right cerebral hemisphere with an enlarged left lateral ventricle. Because a blood test revealed significant increases in prothrombin time (29.3 s) and activated partial thromboplastin time (104.3 s), but not in D-dimer (0.7 μg/ml) at 1 day after birth, he was treated with a daily infusion of fresh frozen plasma for 12 days. At 37 days after birth, he underwent a ventricular-peritoneal shunt (V-P shunt) operation for progressive enlargement of the lateral ventricle. Computed tomography (CT) at 2 months of age showed an enlarged bilateral lateral ventricle and an extremely reduced volume of bilateral frontal white matter (Figures 2G–2I). Blood coagulation was normalized at 7 months. At the 7 months, the individual did not show any head control or rolling, and presented with abnormal posturing and spastic quadriplegia dominant on the left side of his body. With

rehabilitation, he had full-range visual pursuit, a social smile, and incomplete head control. Although his spasticity improved, exaggerated deep tendon reflexes with synergic voluntary movement of the distal part of the extremities were recognized. An EEG at 1 year of age showed no epileptic discharges. His present developmental quotient is below 20. He did not show hematuria, muscular cramps, intracranial aneurysms, or cataracts. His elder sister was found to have an intraventricular hemorrhage two days after birth and underwent a V-P shunt. Her development was almost normal, and internal strabismus was noted. Unfortunately, she died in an accident at the age of four, and so her DNA was unavailable (Figure 1B).

Genomic DNA was isolated from peripheral blood leukocytes according to standard methods. DNA for mutation screening was amplified by illustra GenomiPhi V2 DNA Amplification Kit (GE Healthcare, Buckinghamshire, UK). The DNA of family members of individual 1 was isolated from saliva samples with Oragene (DNA Genotek Inc., Ontario, Canada). Exons 2 to 48 covering the entire *COL4A2* coding region (GenBank accession number NM_001846.2) were examined by high-resolution melting curve (HRM) analysis or directly sequenced (for exon 46). The samples showing an aberrant melting curve pattern in the HRM analysis were sequenced. PCR primers and conditions are shown in Table S1, available online. All the mutations were verified with genomic DNA as a template. Two heterozygous mutations, c.3455G>A (p.Gly1152Asp) in individual 1 and c.3110G>A (p.Gly1037Glu) in individual 2, were identified. Both mutations occur at evolutionary conserved Gly residues in the Gly-X-Y repeats (Figure 1D), suggesting that the two mutations may alter the collagen IV $\alpha1\alpha1\alpha2$ heterotrimers. These mutations were absent in 200 normal Japanese controls, and our evaluation with web-based prediction tools strongly suggested that these substitutions are pathogenic (Table S2). Screening for *COL4A1* mutations was negative for both individuals (data not shown). The c.3455G>A mutation was found in the proband's mother and the maternal uncle, who showed very mild monoparesis of the left upper extremity and congenital left hemiplegia, respectively, and in maternal grandfather who is asymptomatic (Figures 1A and 1B). Therefore the c.3455G>A mutation can be considered as a pathogenic mutation with incomplete penetrance. The c.3110G>A mutation in individual 2 was not found in his parents, indicating that this mutation occurred de novo (Figure 1C).

Here we report two individuals with porencephaly who harbor *COL4A2* mutations. In individual 2, the mutation occurred de novo. It is noteworthy that individual 2's elder sister also suffered from an intraventricular hemorrhage. A coincidental phenocopy in the sister is possible and would be consistent with de novo occurrence of the mutation. Alternatively, the sister might have the same mutation, which could be inherited from either one of the parents with a germline-mosaic mutation, though it was impossible to examine the sister because her sample is unavailable. Thus, with the present data, we concluded that the c.3110G>A mutation occurred de novo. On the other hand, the mutation in individual 1 was inherited from his mildly affected mother. In addition, congenital hemiplegia is observed in familial members of individual 1; the segregation of the c.3455G>A mutation is consistent with a dominant trait with incomplete penetrance. Such incomplete penetrance also has been reported in familial porencephalies with *COL4A1* mutations,[8,9] suggesting that abnormalities of collagen IV $\alpha1\alpha1\alpha2$ heterotrimers may conspire with other risk factors. The porencephalic cyst was unilateral in individual 1 and bilateral in individual 2, who required shunting, indicating variable severities caused by the different *COL4A2* mutations. Most porencephalic cysts caused by *COL4A1* mutations are unilateral;[9] however, Meuwissen et al. recently reported *de novo COL4A1* mutations in sporadic extensive bilateral porencephaly resembling hydranencephaly, indicating similar variable severities caused by *COL4A1* mutations.[10] Thus the involvement of *COL4A1* and *COL4A2* abnormalities should be considered in porencephaly and related pre- and perinatal cerebral hemorrhages, regardless of their severities.

It has been reported that *COL4A1* mutations cause a variety of phenotypes, including porencephaly, infantile hemiplegia, and cerebral small vessel diseases involving both ischemic stroke and intracerebral hemorrhage with radiological features of lacunar infarction, and leukoaraiosis in adult individuals.[9,15–18] The phenotypes in the central nervous system are often accompanied by ocular features (cataracts, retinal vessel tortuosity and hemorrhage, and defects of the anterior segment of the eye), nephropathy, and muscle cramps.[9,16,17] Considering the common pathological mechanism between *COL4A1* and *COL4A2* mutations (abnormalities of collagen IV $\alpha1\alpha1\alpha2$ heterotrimers), *COL4A2* mutations also may be involved in small vessel diseases that can be manifested in adulthood. Supporting this idea, mice lines harboring *Col4A2* point mutations showed cataracts, abnormalities of the lens and the cornea, and cerebral abnormalities.[14] Thus it is important to identify mutations in both *COL4A1* and *COL4A2* in individuals with porencephaly as well as in asymptomatic carriers, for whom the prevention of stroke and genetic counseling are quite important. Identification of pathogenic mutations in individuals with porencephaly is of great interest for obstetricians and pediatricians, and for neurologists working for adult individuals.

In summary, we have identified mutations in *COL4A2* as a genetic cause of both sporadic and familial porencephaly. Our data further support the importance of genetic testing in porencephaly and related pre- and perinatal cerebral hemorrhages for which the genetic predisposition is gradually being uncovered.

Supplemental Data

Supplemental Data include two tables and can be found with this article online at http://www.cell.com/AJHG/.

Acknowledgments

We would like to thank all the individuals and their families for their participation in this study. This work was supported by research grants from the Ministry of Health, Labour and Welfare (K.H., N. Miyake, H.O., M.K., N. Matsumoto, and H.S.), the Japan Science and Technology Agency (N. Matsumoto), the Strategic Research Program for Brain Sciences (N. Matsumoto), and a Grant-in-Aid for Scientific Research on Innovative Areas-(Foundation of Synapse and Neurocircuit Pathology)-from the Ministry of Education, Culture, Sports, Science and Technology of Japan (N. Matsumoto), a Grant-in-Aid for Scientific Research from Japan Society for the Promotion of Science (H.O., N. Matsumoto), a Grant-in-Aid for Young Scientist from Japan Society for the Promotion of Science (H.D., N. Miyake, H.S.) and a grant from the Takeda Science Foundation (N. Miyake and N. Matsumoto). This work has been done at the Advanced Medical Research Center, Yokohama City University, Japan.

Received: September 27, 2011
Revised: November 4, 2011
Accepted: November 17, 2011
Published online: December 29, 2011

Web Resources

The URLs for data presented herein are as follows:

Clustal W, http://www.genome.jp/tools/clustalw/
GenBank, http://www.ncbi.nlm.nih.gov/Genbank/
Online Mendelian Inheritance in Man (OMIM), http://www.omim.org

References

1. Berg, R.A., Aleck, K.A., and Kaplan, A.M. (1983). Familial porencephaly. Arch. Neurol. *40*, 567–569.
2. Govaert, P. (2009). Prenatal stroke. Semin. Fetal Neonatal Med. *14*, 250–266.
3. Hunter, A. (2006). Porencephaly. In Human Malformations and related Anomalies, S. Re and H. Jg, eds. (New York: Oxford University Press), pp. 645–654.
4. Mancini, G.M., de Coo, I.F., Lequin, M.H., and Arts, W.F. (2004). Hereditary porencephaly: clinical and MRI findings in two Dutch families. Eur. J. Paediatr. Neurol. *8*, 45–54.
5. Vilain, C., Van Regemorter, N., Verloes, A., David, P., and Van Bogaert, P. (2002). Neuroimaging fails to identify asymptomatic carriers of familial porencephaly. Am. J. Med. Genet. *112*, 198–202.
6. Moinuddin, A., McKinstry, R.C., Martin, K.A., and Neil, J.J. (2003). Intracranial hemorrhage progressing to porencephaly as a result of congenitally acquired cytomegalovirus infection—an illustrative report. Prenat. Diagn. *23*, 797–800.
7. Gould, D.B., Phalan, F.C., Breedveld, G.J., van Mil, S.E., Smith, R.S., Schimenti, J.C., Aguglia, U., van der Knaap, M.S., Heutink, P., and John, S.W. (2005). Mutations in *Col4a1* cause perinatal cerebral hemorrhage and porencephaly. Science *308*, 1167–1171.
8. Breedveld, G., de Coo, I.F., Lequin, M.H., Arts, W.F., Heutink, P., Gould, D.B., John, S.W., Oostra, B., and Mancini, G.M. (2006). Novel mutations in three families confirm a major role of *COL4A1* in hereditary porencephaly. J. Med. Genet. *43*, 490–495.
9. Lanfranconi, S., and Markus, H.S. (2010). *COL4A1* mutations as a monogenic cause of cerebral small vessel disease: a systematic review. Stroke *41*, e513–e518.
10. Meuwissen, M.E., de Vries, L.S., Verbeek, H.A., Lequin, M.H., Govaert, P.P., Schot, R., Cowan, F.M., Hennekam, R., Rizzu, P., Verheijen, F.W., et al. (2011). Sporadic *COL4A1* mutations with extensive prenatal porencephaly resembling hydranencephaly. Neurology *76*, 844–846.
11. Khoshnoodi, J., Pedchenko, V., and Hudson, B.G. (2008). Mammalian collagen IV. Microsc. Res. Tech. *71*, 357–370.
12. Engel, J., and Prockop, D.J. (1991). The zipper-like folding of collagen triple helices and the effects of mutations that disrupt the zipper. Annu. Rev. Biophys. Biophys. Chem. *20*, 137–152.
13. Gajko-Galicka, A. (2002). Mutations in type I collagen genes resulting in osteogenesis imperfecta in humans. Acta Biochim. Pol. *49*, 433–441.
14. Favor, J., Gloeckner, C.J., Janik, D., Klempt, M., Neuhäuser-Klaus, A., Pretsch, W., Schmahl, W., and Quintanilla-Fend, L. (2007). Type IV procollagen missense mutations associated with defects of the eye, vascular stability, the brain, kidney function and embryonic or postnatal viability in the mouse, Mus musculus: an extension of the *Col4a1* allelic series and the identification of the first two *Col4a2* mutant alleles. Genetics *175*, 725–736.
15. Vahedi, K., and Alamowitch, S. (2011). Clinical spectrum of type IV collagen (COL4A1) mutations: a novel genetic multisystem disease. Curr. Opin. Neurol. *24*, 63–68.
16. Sibon, I., Coupry, I., Menegon, P., Bouchet, J.P., Gorry, P., Burgelin, I., Calvas, P., Orignac, I., Dousset, V., Lacombe, D., et al. (2007). *COL4A1* mutation in Axenfeld-Rieger anomaly with leukoencephalopathy and stroke. Ann. Neurol. *62*, 177–184.
17. Alamowitch, S., Plaisier, E., Favrole, P., Prost, C., Chen, Z., Van Agtmael, T., Marro, B., and Ronco, P. (2009). Cerebrovascular disease related to *COL4A1* mutations in HANAC syndrome. Neurology *73*, 1873–1882.
18. Gould, D.B., Phalan, F.C., van Mil, S.E., Sundberg, J.P., Vahedi, K., Massin, P., Bousser, M.G., Heutink, P., Miner, J.H., Tournier-Lasserve, E., and John, S.W. (2006). Role of COL4A1 in small-vessel disease and hemorrhagic stroke. N. Engl. J. Med. *354*, 1489–1496.

CLINICAL REPORT

AMERICAN JOURNAL OF medical genetics PART A

Early Infantile Epileptic Encephalopathy Associated With the Disrupted Gene Encoding Slit-Robo Rho GTPase Activating Protein 2 (*SRGAP2*)

Hirotomo Saitsu,[1]* Hitoshi Osaka,[2] Shirou Sugiyama,[2] Kenji Kurosawa,[3] Takeshi Mizuguchi,[1] Kiyomi Nishiyama,[1] Akira Nishimura,[1] Yoshinori Tsurusaki,[1] Hiroshi Doi,[1] Noriko Miyake,[1] Naoki Harada,[4] Mitsuhiro Kato,[5] and Naomichi Matsumoto[1]

[1]Department of Human Genetics, Graduate School of Medicine, Yokohama City University, Kanazawa-ku, Yokohama, Japan

[2]Division of Neurology, Clinical Research Institute, Kanagawa Children's Medical Center, Minami-ku, Yokohama, Japan

[3]Division of Medical Genetics, Clinical Research Institute, Kanagawa Children's Medical Center, Minami-ku, Yokohama, Japan

[4]Cytogenetic Testing Group B, Advanced Medical Science Research Center, Mitsubishi Chemical Medience Corporation, Nagasaki, Japan

[5]Faculty of Medicine, Department of Pediatrics, Yamagata University Yamagata, Japan

Received 25 January 2011; Accepted 31 July 2011

We report on a female patient with early infantile epileptic encephalopathy and severe psychomotor disability possessing a de novo balanced translocation t(1;9)(q32;q13). The patient showed clonic convulsions of extremities 2 days after birth. Electroencephalogram (EEG) transiently showed atypical suppression-burst pattern. The seizures evolved to brief tonic spasms, and hypsarrhythmia on EEG was noticed at age of 5 months, indicating the transition to West syndrome. By using fluorescent in situ hybridization (FISH), southern hybridization, and inverse PCR, the translocation breakpoints were successfully determined at the nucleotide level. The 1q32.1 breakpoint was located within a segmental duplication and disrupted the gene encoding Slit-Robo Rho GTPase activating protein 2 (*SRGAP2*). The 9q13 breakpoint was suggested to reside in the heterochromatin region. *Srgap2* has been shown to be specifically expressed in developing brain of rodents, negatively regulate neuronal migration and induce neurite outgrowth and branching. Thus, *SRGAP2* is very likely to play a role in the developing human brain. This is a first report of the *SRGAP2* abnormality associated with early infantile epileptic encephalopathy.

Key words: early infantile epileptic encephalopathy; West syndrome; chromosomal translocation; *SRGAP2*

How to Cite this Article:
Saitsu H, Osaka H, Sugiyama S, Kurosawa K, Mizuguchi T, Nishiyama K, Nishimura A, Tsurusaki Y, Doi H, Miyake N, Harada N, Kato M, Matsumoto N. 2012. Early infantile epileptic encephalopathy associated with the disrupted gene encoding Slit-Robo Rho GTPase activating protein 2 (*SRGAP2*).
Am J Med Genet Part A 158A:199–205.

INTRODUCTION

Many infantile epileptic syndromes show a unique combination of seizure types and electroencephalogram (EEG) findings depending on the patients' age [Kato et al., 2008]. Ohtahara syndrome (OS) and early myoclonic encephalopathy (EME) are characterized by early onset seizures mainly in neonatal period, and suppression-burst pattern on EEG, though their initial seizure type is different [Djukic et al., 2006; Ohtahara and Yamatogi, 2006]. Both OS and EME can progress to the West syndrome phenotype age-dependently, which is characterized by brief tonic spasms, a specific EEG pattern called hypsarrhythmia [Kato, 2006], in 75% and 41% of cases, respectively [Djukic et al., 2006; Ohtahara and Yamatogi, 2006]. The three epileptic syndromes (OS, EME, and West syndrome) are generally intractable and show the arrest of psychomotor development [Djukic et al., 2006; Kato, 2006; Ohtahara and Yamatogi, 2006]. Brain malformations and metabolic disorders were found as underlying causes of the three syndromes, but

Grant sponsor: Ministry of Health, Labour and Welfare; Grant sponsor: Japan Society for the Promotion of Science; Grant sponsor: Yokohama Foundation for Advancement of Medical Science; Grant sponsor: Japan Epilepsy Research Foundation; Grant sponsor: Naito Foundation.
*Correspondence to:
Dr. Hirotomo Saitsu, Department of Human Genetics, Yokohama City University Graduate School of Medicine, Fukuura 3-9, Kanazawa-ku, Yokohama 236-0004, Japan. E-mail: hsaitsu@yokohama-cu.ac.jp
Published online 21 November 2011 in Wiley Online Library (wileyonlinelibrary.com).
DOI 10.1002/ajmg.a.34363

many idiopathic or cryptogenic cases remain etiologically unexplained. Recently, several causative genes have been reported: *ARX* in OS and West syndrome, *CDKL5* in West syndrome, *STXBP1* in OS, *SLC25A22* in EME [Stromme et al., 2002; Kalscheuer et al., 2003; Weaving et al., 2004; Molinari et al., 2005; Kato et al., 2007; Saitsu et al., 2008]. Of note, mutations in *ARX* have been found in both OS and West syndrome phenotypes, suggesting a common pathological seizure mechanism between them. However, there are still large numbers of cases remaining to be elucidated. Identification of new causative genes is absolutely necessary for further understanding of infantile epileptic syndromes.

The Slit-Robo signaling controls the neuronal migration and axonal guidance [Brose et al., 1999; Li et al., 1999; Wu et al., 1999], both of which are dependent on cytoskeletal reorganization. The family of Rho-GTPases, including Rac, Cdc42, and Rho, plays important roles in regulating cytoskeletal dynamics [Hall, 1998]. Rho-GTPases alternate between active (GTP-bound) and inactive (GDP-bound) conformation. The activities of Rho GTPases are tightly and antagonistically regulated by Guanine nucleotide exchange factors (GEFs) and GTPase activating proteins (GAPs): GEFs catalyze nucleotide exchange and mediate activation, while GAPs increase the intrinsic GTPase activities to promote GTP hydrolysis, leading to inactivation [Lamarche and Hall, 1994]. Slit-Robo Rho GTPase activating proteins (SRGAPs) were identified as a family of GAP proteins which bind to the intracellular domain of Robo [Wong et al., 2001]. Three family members (SRGAP1-3) specifically expressed in developing brain of rodents [Wong et al., 2001; Yao et al., 2008; Bacon et al., 2009]. Recent studies suggested that SRGAPs are involved in neuronal development. SRGAP1 protein is required for Slit-mediated repulsion of migratory cells from the anterior subventricular zone of the forebrain by blocking Cdc42 activity [Wong et al., 2001]. Functional disruption of SRGAP3 protein is associated with severe mental retardation in 3p-syndrome [Endris et al., 2002]. Moreover, it has been reported that SRGAP2 negatively regulates neuronal migration and induces neurite outgrowth and branching [Guerrier et al., 2009].

Here, we present a patient with infantile epileptic encephalopathy and profound psychomotor delay with a de novo reciprocal translocation t(1;9)(q32;q13), disrupting the *SRGAP2* gene. Detailed genomic analysis is presented.

CLINICAL REPORT

The 5-year-old girl is a product of unrelated healthy parents. She was born at term without asphyxia after an uneventful pregnancy. She showed apnea twice at day 1. Clonic convulsions of extremities started at day 2. Initial EEG performed at 10-day was reported as normal. Subsequently, myoclonus, which was easily induced by stimulation, was observed. Ictal EEG during myoclonus did not indicate that it was an electronical convulsion. Clonic convulsions were increased at 2 months of age when atypical suppression-burst pattern was transiently observed (Fig. 1A). Her seizures were controlled by combination of vitamin B6, zonisamide, phenobarbital, and KBr, but myoclonus continued. Brain magnetic resonance imaging (MRI) showed cortical atrophy and thin corpus callosum at 2 months of age (Fig. 1C–E). West syndrome was diagnosed at 5 months of age by intellectual disability without head control, series of tonic-spasms, and hypsarrhysmia on EEG (Fig. 1B).

MATERIALS AND METHODS

Molecular Cytogenetic Analysis

G-banded chromosomes of peripheral lymphocytes were analyzed. Fluorescence in situ hybridization (FISH) was performed using peripheral lymphocytes. Labeling, hybridization, wash, and image acquisition were performed as previously described [Saitsu et al., 2008]. RPCI-11 BAC clones and approximately 10-kb probes amplified by long PCR using LA Taq polymerase (Takara Bio, Otsu, Japan) were used as probes. Primer information is available on request.

GeneChip Human Mapping 250K *Nsp*I Array

Genomic DNA obtained from peripheral blood leukocytes were used for microarray analysis. Experimental procedures were performed according to the manufacturer's protocol with slight modification (fragmentation time was shortened to 25 min). Call rate was 89.5%. Copy number alterations were analyzed by using CNAG2.0 [Nannya et al., 2005].

Cloning of Translocation Breakpoints

The 1q32.1 translocation breakpoint was analyzed by Southern hybridization using *Eco*RI- and *Pst*I-digested patient DNA. Her parental DNAs were also analyzed. Probes were synthesized by PCR DIG probe synthesis kit (Roche, Basel, Switzerland) using RP11-134f21 DNA as a template. Primer information is available on request. Hybridization, washing and detection of probes were done according to the manufacturer's protocol. Images were captured on FluorChem (Alpha Innotech, San Leandro, CA). After identification of aberrant DNA fragments by Southern hybridization, size fractioning of electrophoresed *Eco*RI- and *Pst*I-digested DNA of the patient was performed using QIAEXII Gel extraction kit (Qiagen, Valencia, CA) in order to obtain der(1) and der(9) translocation junction fragments, respectively. The collected DNA was self-ligated by Ligation high (Toyobo, Osaka, Japan), ethanol precipitated and dissolved in 20 μl EB buffer (Qiagen). Inverse PCR was performed in 25 μl of volume, containing 2 μl ligated DNA, 1× LA PCR bufferII, 2.5 mM $MgCl_2$, 0.4 mM each dNTP, 0.5 μM each primer, and 1.25 U LA Taq polymerase (Takara Bio). Primers were listed below: *Eco*RI-forward, 5′-GAAATGGCCTGGCTTGGTT-GCTAT-3′; *Eco*RI-reverse, 5′-CACTGAAGCTGCCCTTGAGAA-GTGA-3′; *Pst*I-forward, 5′-TTTCCCTCCATGATTCCTCTCT-GCT-3′; *Pst*I-reverse, 5′-CCAGGACAGCGTCTCACTCTCCATA-3′. Negative controls only used either forward or reverse primer. The PCR product was purified with ExoSAP (USB Co., Cleveland, OH) and sequenced for both forward and reverse strands with BigDye Terminator chemistry ver. 3 according to the standard protocol (Applied Biosystems, Foster city, CA). After breakpoint sequences were determined, breakpoint-specific primers for both der(1) and der(9) translocation junctions were designed: der(1)-forward, 5′-CCAAGGAATTGGGATCTCTGGGTCT -3′; der(1)-reverse, 5′-CATTCCATTCCATTCCCCTGCAC -3′ (1,098-bp);

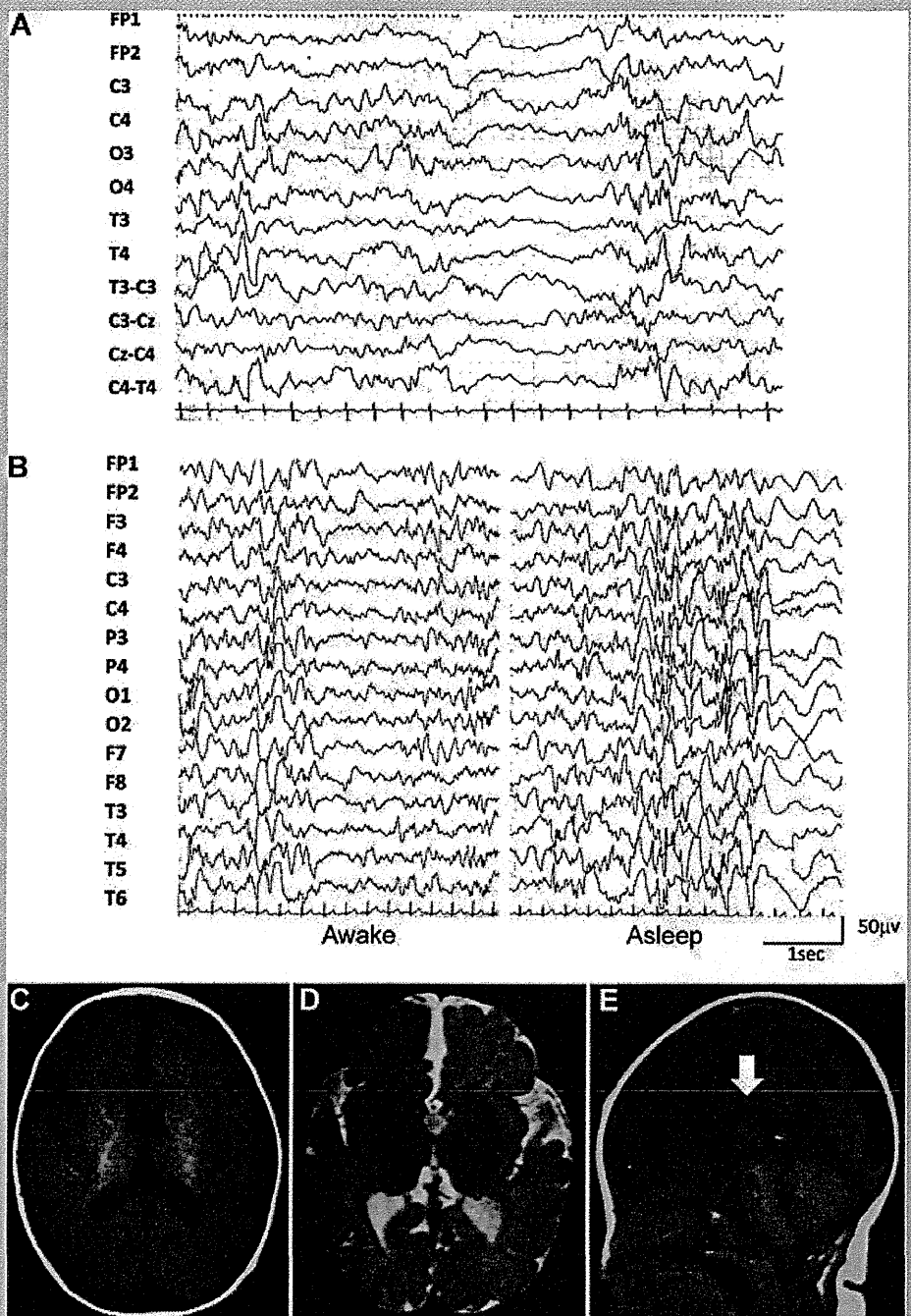

FIG. 1. EEG and brain MRI of the patient. A: Interictal high-voltage bursts alternate with low amplitude suppression phases at an approximately regular rate in both awake and asleep states at age of 2 months. Suppression phases do not exhibit "almost flat pattern" as typical suppression-burst pattern. B: Interictal EEG at 5 months shows multifocal spikes at awake (left), and high-voltage slow rhythm superimposed with irregular spikes; hypsarrhythmia at sleep with some periodicity (right). C,D: Brain MRI T1- (C) and T2-weighted (D) axial images show mild cortical atrophy with normal myelination. E: Sagital brain T1-weighted image shows thin corpus callosum (arrow)

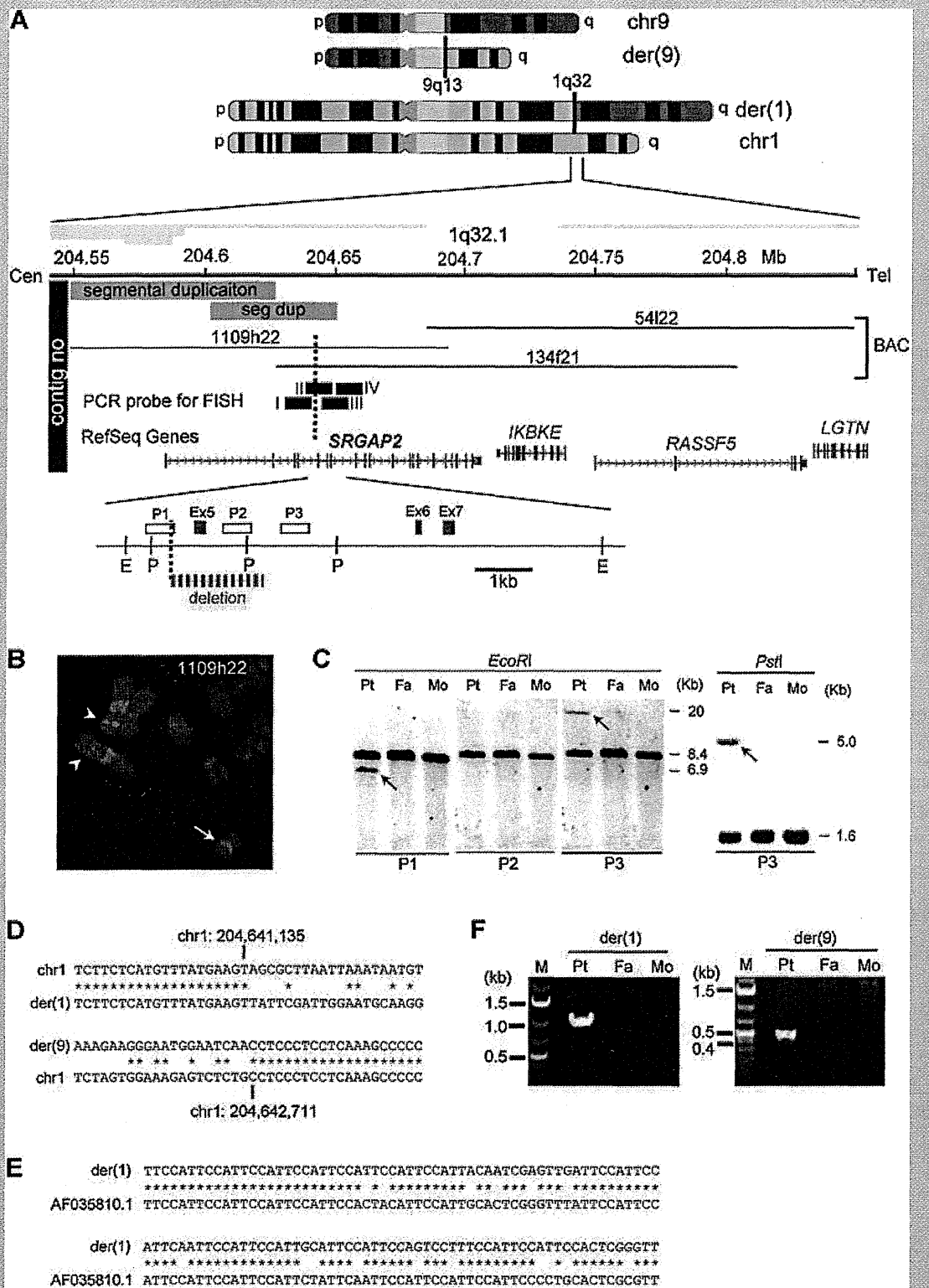
A
chr9
der(9)
der(1)
chr1
9q13
1q32
1q32.1
204.55
204.6
204.65
204.7
204.75
204.8 Mb
Cen
Tel
segmental duplicaiton
seg dup
54l22
1109h22
134f21
BAC
contig no
PCR probe for FISH
RefSeq Genes
SRGAP2
IKBKE
RASSF5
LGTN
P1
Ex5
P2
P3
Ex6
Ex7
deletion
1kb
B
1109h22
C
EcoRI
PstI
Pt Fa Mo
(Kb)
20
8.4
6.9
5.0
1.6
P1
P2
P3
D
chr1: 204,641,135
chr1 TCTTCTCATGTTTATGAAGTAGCGCTTAATTAAATAATGT
der(1) TCTTCTCATGTTTATGAAGTTATTCGATTGGAATGCAAGG
der(9) AAAGAAGGGAATGGAATCAACCTCCCTCCTCAAAGCCCCC
chr1 TCTAGTGGAAAGAGTCTCTGCCTCCCTCCTCAAAGCCCCC
chr1: 204,642,711
F
der(1)
der(9)
M Pt Fa Mo
(kb)
1.5
1.0
0.5
0.4
E
der(1) TTCCATTCCATTCCATTCCATTCCATTCCATTCCATTACAATCGAGTTGATTCCATTCC
AF035810.1 TTCCATTCCATTCCATTCCATTCCACTACATTCCATTGCACTCGGGTTTATTCCATTCC
der(1) ATTCAATTCCATTCCATTGCATTCCATTCCAGTCCTTTCCATTCCATTCCACTCGGGTT
AF035810.1 ATTCCATTCCATTCCATTCTATTCAATTCCATTCCATTCCATTCCCCTGCACTCGCGTT

der(9)-forward, 5′-GGAAAGGAATGGAATGAAATCAACGCG-3′; der(9)-reverse, 5′-CCAGGACAGCGTCTCACTCTCCATA-3′ (495-bp). Junction fragments were amplified by PCR using these primer-sets on DNAs of the patient and her parents.

RESULTS

G-banded chromosomal analysis revealed a balanced translocation t(1;9)(q32;q13). Her parents showed a normal karyotype (data not shown), indicating that the translocation occurred de novo. Subsequent FISH analysis demonstrated that the breakpoint in chromosome 1 was covered by the clones, RP11-1109h22 and 134f21, showing signals all on normal chromosome 1 and derivatives chromosomes 1 and 9 (Fig. 2A,B). The overlapping region of these two clones was localized within the *SRGAP2* locus (Fig. 2A). The 5′-part of *SRGAP2* transcript was not mapped in the Human Genome browser (both in NCBI Build 36.1/hg18 and GRCh37/hg19 assembly) because the genomic contigs covering the immediately upstream regions of *SRGAP2* gene were absent. Thus, we described the putative exon number based on the order of mappable exons to the existing genomic database. The breakpoint was further narrowed down by FISH analysis using long PCR products as probes (Fig. 2A). Probe II showed weak but clear signals all in on chromosome 1, and derivative chromosomes 1 and 9, suggesting that the breakpoint was located within probe II (data not shown). It was of note that the probe II is associated with a segmental duplication (Fig. 2A). Southern hybridization analysis using probes P1 and P3 detected different aberrant bands only in the patient (Fig. 2A,C), indicating that the 1q32 breakpoint was located at the region between the two probes. P2 did not show any aberrant bands in Southern analysis, suggesting that a small deletion may have occurred near the breakpoint (Fig. 2A,C). Inverse PCR [Triglia et al., 1988] on *Eco*RI- and *Pst*I-digested DNA was successful in obtaining der(1) and der(9) breakpoint-junction fragments, respectively. Sequence analysis showed that the 1q32 translocation breakpoint was located within the putative intron 5 of *SRGAP2*, and exon 5 was completely deleted (Fig. 2A). Sequences of the 9q13 breakpoint were not uniquely mapped to reference sequences. However, sequences of 3′-end of the der(1) junction fragment (approximately 6.1-kb apart from the breakpoint) were similar to satellite 3 sequences (GeneBank accession number AF035810.1) (Fig. 2E), suggesting that 9q13 breakpoint was located in the heterochromatin region. Breakpoint-specific PCR analysis of the patient and her parents confirmed that the rearrangements occurred de novo (Fig. 2F). To check genomic copy number alterations accompanied by the rearrangement, GeneChip Human Mapping 250K *Nsp*I (Affymetrix, Santa Clara, CA) was performed. Besides two known copy number variations, no other imbalances were detected (data not shown).

DISCUSSION

SRGAP2 is a member of Slit-Robo Rho GTPase activating proteins with three domains: an N-terminal F-BAR domain, a RhoGAP domain, and an SH3 domain [Wong et al., 2001; Guerrier et al., 2009]. There are three variants of *SRGAP2* transcripts in humans: variant 1 (GenBank accession number NM_015326.2), variant 2 (GenBank accession number NM_001042758.1), and variant 3 (GenBank accession number NM_001170637.1). In all three variants, the coding proteins commonly possess F-BAR, RhoGAP, and SH3 domains except for an amino acid deletion in F-BAR domain in variant 2. Mouse *Srgap2* is expressed in the entire developing cortex including proliferative zones and postmitotic regions [Bacon et al., 2009; Guerrier et al., 2009]. It has been reported that the SRGAP2 protein negatively regulates neuronal migration and induce neurite outgrowth and branching through its F-BAR domain [Guerrier et al., 2009]. In addition, GAP activity of the SRGAP2 protein specifically downregulate Rac1 [Guerrier et al., 2009]. Mutations in *ARHGEF6*, Rac1/Cdc42 specific GEF, cause X-linked mental retardation [Kutsche et al., 2000]. Moreover, mutation and/or disruption of *OPHN1* and *SRGAP3*, both encoding Rac1-GAPs, are associated with severe mental retardation [Billuart et al., 1998; Endris et al., 2002], indicating the importance of Rac1 regulation in human brain development. Thus, SRGAP2 is likely to play important roles in developing brain in humans through the ability of the F-BAR and RhoGAP domains. It would be interesting to analyze

FIG. 2. Genomic characterization of t(1;9)(q32;q13). A: Schematic representation of the reciprocal translocation, t(1;9)(q32;q13) (top). A summarized physical map covering the 1q32.1 translocation breakpoint is indicated (middle). RP11-1109h22 and 134f21, and PCR probe II span the translocation breakpoint (longitudinal dashed line) in association with the segmental duplication. Four RefSeq genes, including *SRGAP2* spanning the breakpoint, are presented. Note that absence of genomic contigs of the immediately upstream region of the *SRGAP2* gene. More detailed maps are shown (bottom). A partial restriction map (E, *Eco*RI; P, *Pst*I), probes for southern hybridization (P1–P3), and putative exons 5–7 of *SRGAP2* are indicated. Translocation breakpoint (longitudinal dashed line) accompanied with a 1,575-bp deletion encompassing exon 5 of *SRGAP2* (red thick dashed line) are located between P1 and P3. B: FISH analysis using RP11-1109h22 as a probe showed clear signals on chromosome 1, and der(1) (white arrowheads) and der(9) chromosomes (white arrow). Cross-hybridization was also observed to segmental duplications located at pericentric regions of chromosome 1 and derivative chromosome 1. C: Southern hybridization using probes P1, P2, and P3 on genomic DNAs of the patient and her parents. Arrow shows aberrant bands specific to the patient (not observed in parental DNA). Pt, patient; Fa, father; Mo, mother. D: Breakpoint junction sequences of der(1) and der(9). In upper part, top and bottom sequence strands show chromosome 1 and derivative chromosome 1 sequences, respectively. In lower part, top and bottom strands show derivative chromosome 9 and normal chromosome 1 sequences, respectively. Breakpoint positions are marked with small longitudinal lines based on the UCSC genome browser coordinate (version Mar. 2006). Asterisks indicate nucleotides identical to normal chromosomes. E: Sequences of the 3′-end of the der(1) junction fragment. Top and bottom sequence strands show der(1) and satellite 3 sequences, respectively, showing homology between two sequences. F: Breakpoint-specific PCR analysis of the patient's family. Primers specific to der(1) and der(9) breakpoints could successfully amplify 1,098- and 495-bp products, respectively, only from the patient (Pt), indicating the translocation occurred de novo. M, size marker; Fa, father; Mo, mother.

SRGAP2 in a large cohort of patients presenting with early epileptic encephalopathy including West syndrome. Although full-length *SRGAP2* transcripts (functional), which include sequences of putative exons 1–20 at 1q32.1, have been deposited in GeneBank, 5′-part of the *SRGAP2* transcript is not mapped in the Human Genome browser. Furthermore, seven exons of *SRGAP2* were again mapped to two separated segmental duplications at 1q21.1 and 1p11.2 with sequence similarities of 99.29% and 99.30%, respectively (Fig. 2A). This complex genomic structure interfered with full-blown mutation screening especially for the 1,356-bp coding region including the F-BAR domain. A microdeletion within two separate segmental duplications in *SRGAP2* locus has been found in 2 out of 90 Yoruban individuals (presumably with normal phenotype) from the HapMap Project using custom high-density oligonucleotide arrays [Matsuzaki et al., 2009]. However, it is uncertain whether they could confirm the precise locations of the deletions by another method. Thus, there remains a possibility that the deletion actually ocurred at highly homologous genomic segments located at 1q21.1 and 1p11.2. Further descriptions about aberrations of the *SRGAP2* gene will be required for establishing in a causative role in early infantile epileptic encephalopathy.

The 9q13 breakpoint is likely to reside within the heterochromatic region. It is possible that some genes adjacent to 1q32.1 breakpoint would suffer from gene silencing by the position effect. *IKBKE* is an IKK (inhibitor of nuclear factor kappaB kinase)-related kinase that is essential for interferon-inducible antiviral transcriptional response [Tenoever et al., 2007]. *Ikbke* knockout mice are protected from high-fat diet-induced obesity, chronic inflammation in liver and fat, hepatic steatosis, and whole-body insulin resistance [Chiang et al., 2009]. However, neurological abnormalities have never been reported. *RASSF5* is a member of the Ras association domain family. A crutial role in the integrin-mediated adhesion and migration of lymphocytes and dendritic cells has been shown in *Rassf5*-deficient mice, but neurological abnormalities have never been mentioned [Katagiri et al., 2004]. Thus, *IKBKE* and *RASSF5*, two adjacent genes to *SRGAP2*, are less likely to be involved in infantile epileptic encephalopathy.

In conclusion, we described a patient with early infantile epilepsitic encephalopathy, carrying a de novo reciprocal translocation disrupting the *SRGAP2* gene. Clonic convulsions and atypical suppression-burst patterns on EEG at early infantile period did not fit into either OS or EME. However, the seizures became brief tonic spasms, and hypsarrhythmia on EEG was noticed, indicating transition to West syndrome. Disruption of *SRGAP2* may be related to West syndrome which has heterogeneous backgrounds [Kato, 2006].

ACKNOWLEDGMENTS

We would like to thank the patient and her families for their participation in this study. This work was supported by Research Grants from the Ministry of Health, Labour and Welfare (H.S. and N. Matsumoto), Grant-in-Aid for Scientific Research from Japan Society for the Promotion of Science (N. Matsumoto), Grant-in-Aid for Young Scientist from Japan Society for the Promotion of Science (H.S.), Research Promotion Fund from Yokohama Foundation for Advancement of Medical Science (H.S.), Research Grants from the Japan Epilepsy Research Foundation (H.S.), and Research Grant from Naito Foundation (N. Matsumoto).

REFERENCES

Bacon C, Endris V, Rappold G. 2009. Dynamic expression of the Slit-Robo GTPase activating protein genes during development of the murine nervous system. J Comp Neurol 513:224–236.

Billuart P, Bienvenu T, Ronce N, des Portes V, Vinet MC, Zemni R, Roest Crollius H, Carrie A, Fauchereau F, Cherry M, Briault S, Hamel B, Fryns JP, Beldjord C, Kahn A, Moraine C, Chelly J. 1998. Oligophrenin-1 encodes a rhoGAP protein involved in X-linked mental retardation. Nature 392:923–926.

Brose K, Bland KS, Wang KH, Arnott D, Henzel W, Goodman CS, Tessier-Lavigne M, Kidd T. 1999. Slit proteins bind Robo receptors and have an evolutionarily conserved role in repulsive axon guidance. Cell 96:795–806.

Chiang SH, Bazuine M, Lumeng CN, Geletka LM, Mowers J, White NM, Ma JT, Zhou J, Qi N, Westcott D, Delproposto JB, Blackwell TS, Yull FE, Saltiel AR. 2009. The protein kinase IKKepsilon regulates energy balance in obese mice. Cell 138:961–975.

Djukic A, Lado FA, Shinnar S, Moshe SL. 2006. Are early myoclonic encephalopathy (EME) and the Ohtahara syndrome (EIEE) independent of each other? Epilepsy Res 70:S68–S76.

Endris V, Wogatzky B, Leimer U, Bartsch D, Zatyka M, Latif F, Maher ER, Tariverdian G, Kirsch S, Karch D, Rappold GA. 2002. The novel Rho-GTPase activating gene MEGAP/ srGAP3 has a putative role in severe mental retardation. Proc Natl Acad Sci USA 99:11754–11759.

Guerrier S, Coutinho-Budd J, Sassa T, Gresset A, Jordan NV, Chen K, Jin WL, Frost A, Polleux F. 2009. The F-BAR domain of srGAP2 induces membrane protrusions required for neuronal migration and morphogenesis. Cell 138:990–1004.

Hall A. 1998. Rho GTPases and the actin cytoskeleton. Science 279: 509–514.

Kalscheuer VM, Tao J, Donnelly A, Hollway G, Schwinger E, Kubart S, Menzel C, Hoeltzenbein M, Tommerup N, Eyre H, Harbord M, Haan E, Sutherland GR, Ropers HH, Gecz J. 2003. Disruption of the serine/ threonine kinase 9 gene causes severe X-linked infantile spasms and mental retardation. Am J Hum Genet 72:1401–1411.

Katagiri K, Ohnishi N, Kabashima K, Iyoda T, Takeda N, Shinkai Y, Inaba K, Kinashi T. 2004. Crucial functions of the Rap1 effector molecule RAPL in lymphocyte and dendritic cell trafficking. Nat Immunol 5:1045–1051.

Kato M. 2006. A new paradigm for West syndrome based on molecular and cell biology. Epilepsy Res 70:S87–S95.

Kato M, Saitoh S, Kamei A, Shiraishi H, Ueda Y, Akasaka M, Tohyama J, Akasaka N, Hayasaka K. 2007. A longer polyalanine expansion mutation in the ARX gene causes early infantile epileptic encephalopathy with suppression-burst pattern (Ohtahara syndrome). Am J Hum Genet 81: 361–366.

Kato M, Saitoh S, Kamei A, Shiraishi H, Ueda Y, Akasaka M, Tohyama J, Akasaka N, Hayasaka K., 2008. Genetic etiology of age-dependent epileptic encephalopathy in infancy: Longer polyalanine expansion in ARX causes earlier onset and more severe phenotype. In: Takahashi T, Fukuyama Y, editors. Biology of seizure susceptibility in developing brain. Montrouge, Paris: John Libbey Eurotext. pp. 75–86.

Kutsche K Yntema H Brandt A Jantke I Nothwang HG Orth U Boavida MG David D Chelly J Fryns JP Moraine C Ropers HH Hamel BC van Bokhoven H Gal A 2000 Mutations in ARHGEF6 encoding a guanine nucleotide exchange factor for Rho GTPases in patients with X-linked mental retardation Nat Genet 26:247–250.

Lamarche N, Hall A. 1994. GAPs for rho-related GTPases. Trends Genet 10:436–440.

Li HS, Chen JH, Wu W, Fagaly T, Zhou L, Yuan W, Dupuis S, Jiang ZH, Nash W, Gick C, Ornitz DM, Wu JY, Rao Y. 1999. Vertebrate slit, a secreted ligand for the transmembrane protein roundabout, is a repellent for olfactory bulb axons. Cell 96:807–818.

Matsuzaki H, Wang PH, Hu J, Rava R, Fu GK. 2009. High resolution discovery and confirmation of copy number variants in 90 Yoruba Nigerians. Genome Biol 10:R125.

Molinari F, Raas-Rothschild A, Rio M, Fiermonte G, Encha-Razavi F, Palmieri L, Palmieri F, Ben-Neriah Z, Kadhom N, Vekemans M, Attie-Bitach T, Munnich A, Rustin P, Colleaux L. 2005. Impaired mitochondrial glutamate transport in autosomal recessive neonatal myoclonic epilepsy. Am J Hum Genet 76:334–339.

Nannya Y, Sanada M, Nakazaki K, Hosoya N, Wang L, Hangaishi A, Kurokawa M, Chiba S, Bailey DK, Kennedy GC, Ogawa S. 2005. A robust algorithm for copy number detection using high-density oligonucleotide single nucleotide polymorphism genotyping arrays. Cancer Res 65: 6071–6079.

Ohtahara S, Yamatogi Y. 2006. Ohtahara syndrome: With special reference to its developmental aspects for differentiating from early myoclonic encephalopathy. Epilepsy Res 70:S58–S67.

Saitsu H, Kato M, Mizuguchi T, Hamada K, Osaka H, Tohyama J, Uruno K, Kumada S, Nishiyama K, Nishimura A, Okada I, Yoshimura Y, Hirai S, Kumada T, Hayasaka K, Fukuda A, Ogata K, Matsumoto N. 2008. De novo mutations in the gene encoding STXBP1 (MUNC18-1) cause early infantile epileptic encephalopathy. Nat Genet 40:782–788.

Stromme P, Mangelsdorf ME, Shaw MA, Lower KM, Lewis SM, Bruyere H, Lutcherath V, Gedeon AK, Wallace RH, Scheffer IE, Turner G, Partington M, Frints SG, Fryns JP, Sutherland GR, Mulley JC, Gecz J. 2002. Mutations in the human ortholog of Aristaless cause X-linked mental retardation and epilepsy. Nat Genet 30:441–445.

Tenoever BR, Ng SL, Chua MA, McWhirter SM, Garcia-Sastre A, Maniatis T. 2007. Multiple functions of the IKK-related kinase IKKepsilon in interferon-mediated antiviral immunity. Science 315:1274–1278.

Triglia T, Peterson MG, Kemp DJ. 1988. A procedure for in vitro amplification of DNA segments that lie outside the boundaries of known sequences. Nucleic Acids Res 16:8186.

Weaving LS, Christodoulou J, Williamson SL, Friend KL, McKenzie OL, Archer H, Evans J, Clarke A, Pelka GJ, Tam PP, Watson C, Lahooti H, Ellaway CJ, Bennetts B, Leonard H, Gecz J. 2004. Mutations of CDKL5 cause a severe neurodevelopmental disorder with infantile spasms and mental retardation. Am J Hum Genet 75:1079–1093.

Wong K, Ren XR, Huang YZ, Xie Y, Liu G, Saito H, Tang H, Wen L, Brady-Kalnay SM, Mei L, Wu JY, Xiong WC, Rao Y. 2001. Signal transduction in neuronal migration: Roles of GTPase activating proteins and the small GTPase Cdc42 in the Slit-Robo pathway. Cell 107:209–221.

Wu W, Wong K, Chen J, Jiang Z, Dupuis S, Wu JY, Rao Y. 1999. Directional guidance of neuronal migration in the olfactory system by the protein Slit. Nature 400:331–336.

Yao Q, Jin W-L, Wang Y, Ju G. 2008. Regulated shuttling of Slit-Robo-GTPase activating proteins between nucleus and cytoplasm during brain development. Cell Mol Neurobiol 28:205–221.

CLINICAL GENETICS An International Journal of Genetics, Molecular and Personalized Medicine

Clin Genet 2011: 80: 293–296
Printed in Singapore. All rights reserved

CLINICAL GENETICS
doi: 10.1111/j.1399-0004.2011.01644.x

Letter to the Editor

A novel homozygous mutation of *DARS2* may cause a severe LBSL variant

To the Editor:

Leukoencephalopathy with brain stem and spinal cord involvement, and lactate elevation (LBSL, MIM #611105) is an autosomal recessive disorder with an early childhood-to-adolescence onset. In 2003, van der Knaap et al. originally described LBSL, which is characterized by slowly progressive pyramidal, cerebellar, and dorsal column dysfunction with increased white matter lactate levels in magnetic resonance (MR) spectroscopy (1). Since the first discovery that LBSL is caused by mutations of the *DARS2* gene-encoding mitochondrial aspartyl-tRNA synthetase (MtAspRS) (2), *DARS2* mutations have been found in all the patients described (2–5), but none of them showed a homozygous mutation (all are compound heterozygotes), suggesting that the activity of mutant MtAspRS homodimers may be incompatible with human life (2, 5). Here, we describe, for the first time, a consanguineous family with a homozygous *DARS2* mutation.

Materials and methods

We analyzed a consanguineous family including three affected children diagnosed with leukoencephalopathy (Fig. 1a and Table 1). The proband (II-2) developed truncal ataxic gait at 3 years old. Her affected sister (II-3) and brother (II-4) also showed truncal ataxia at 6 and 11 months, respectively. All cases were presented with horizontal nystagmus, slurring speech, ataxic gait, muscle tonus abnormality, hypo- or hyperreflexia, and tremor as well as mental retardation. II-2 at age 21 years could slowly speak one or two words. Peripheral muscles atrophy, weakness and joints contractures in extremities, loss of deep tendons reflex and disturbed deep sensation were noted. II-3 and II-4 died of pneumonia at age 8 years and respiratory failure at age 2 years, respectively. Although there were differences in MR imaging characteristics from classical LBSL, there were also striking similarities. In our patients, the involvement of the cerebral and cerebellar white matter was more diffused and severe than in classical LBSL, but the affected brain stem and spinal cord tracts were the same (Fig. 1b and Table 1).

Linkage analysis and direct sequencing of *DARS2* were performed as previously reported (6). Immunoblotting was carried out using antihuman DARS2 antibody (ab69336, Abcam, Cambridge, UK) and anti-cytochrome *c* oxidase (COX) IV antibody (ab16056, Abcam).

Results

Homozygosity mapping of this consanguineous family revealed the largest 8.5 Mb homozygous region at chromosome 1q25.1 with the maximum LOD score of 1.329. Five additional microsatellite markers showed the consistent result (Fig. 1a). Within this region, *DARS2* gene was highlighted as the primary target as it was causative for the LBSL. We found that all affected children possessed homozygous, and parents and an unaffected sib had the heterozygous intronic change at 22 base pairs upstream of exon 3 (c.228-22T>A), respectively. This change was not observed in 395 controls. We examined its mutational effect by reverse transcriptase-polymerase chain reaction (RT-PCR) using mRNA of lymphoblastoid cell lines (LCLs) derived from the proband, her father (a carrier) and a normal control. A shorter PCR fragment which lacked the entire exon 3 was confirmed by sequencing (Fig. 1c,d). Furthermore, wild-type *DARS2* mRNA and MtAspRS protein were significantly decreased in proband's LCL (Fig. 1e,f). Other genes within the 1q25.1 region have not been checked.

Discussion

We found a novel homozygous mutation of *DARS2* in a diffuse leukoencephalopathy, which may be an LBSL variant. This change resulted in the decrease of normal protein level and may have contributed to this disease. Two possibilities for the increased severity are considered: (i) a

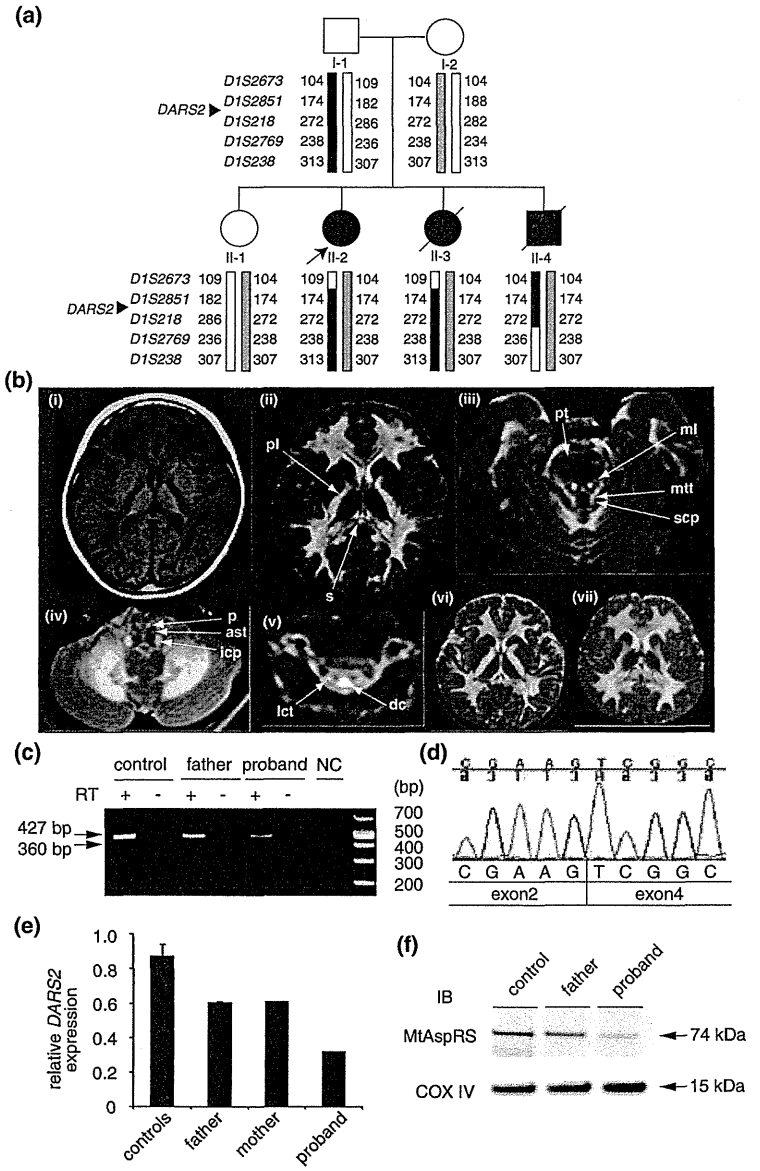

Fig. 1. Identification of a homozygous *DARS2* mutation causing abnormal splicing. (**a**) Haplotype analysis of the family. The black and gray bars represent disease alleles. The *DARS2* gene is located in between *D1S2851* and *D1S218*. (**b**) Magnetic resonance (MR) images of central nervous system in the proband (II-2) at 5 years (i–v), II-3 at 5 years (vi) and II-4 at 1 year and 4 months of age (vii). T_1-weighted (i) and T_2-weighted (T_2) (ii) images of cerebrum. The cerebral white matter was diffusely and severely affected, while the cerebral white matter involvement is less severe and more limited in extent in leukoencephalopathy with brain stem and spinal cord involvement, and lactate elevation with sparing of the U-fibers. Inhomogeneous signal abnormalities were observed in the posterior limb (pl) of the internal capsule and the splenium (s) of the corpus callosum. (iii) T_2 image at the level of the pons. The abnormal high-intensity signals were observed in pyramidal tracts (pt), medial lemniscus (ml), mesencephalic trigeminal tracts (mtt) and superior cerebellar peduncles (scp). (iv) T_2 image at the level of medulla. The pyramids (p), anterior spinocerebellar tracts (ast) and inferior cerebellar peduncles (icp) were affected. (v) T_2 image at the level of the cervical spinal cord. The dorsal columns (dc) and lateral corticospinal tracts (lct) showed abnormal signals. II-3 (vi) and II-4 (vii) showed the similar MR images as the proband. (**c**) RT-PCR using cDNA extracted from LCLs of a normal control, father and the proband. A shorter fragment (360 bp) in addition to a normal product (427 bp) was seen in father and the proband. (**d**) Electropherogram of the shorter fragment showing skipping of exon 3. (**e**) Relative expression of wild-type *DARS2* mRNA compared to β-actin mRNA in LCLs were determined by quantitative real-time RT-PCR using TaqMan Gene Expression Assays (Applied Biosystems, Bedford, MA). The relative *DARS2* expression was analyzed using TaqMan Probe (Applied Biosystems, Hs01016215_m1 for *DARS2* and 4326135E for β-actin as a control). Levels are shown for three controls, parents and the proband based on the calibration curve method using an independent control. Average of duplicated experiments is shown as black bars with the standard error of means. The significant decreased expression of *DARS2* mRNA in the proband was recognized compared to that in three controls ($p < 0.001$, one-way analysis of variance with Bonferroni's multiple comparison test). (**f**) Mitochondrial aspartyl-tRNA synthetase (MtAspRS) protein is expressed in normal control and father as a carrier (fainter), but only weakly recognized in the proband. Cyclooxygenase IV was used as a loading control for the mitochondrial fraction.

Table 1. MRI criteria for LBSL and clinical features of patients

Diagnostic criteria	Case 1	Case 2	Case 3
Major criteria			
Signal abnormalities in			
1. the cerebral white matter, either inhomogeneous and spotty or homogeneous and confluent, sparing the U-fibers	±[a]	±[a]	±[a]
2. the dorsal columns and lateral corticospinal tracts of the spinal cord. (visualization of such abnormalities in the cervical spinal cord suffices)	+	n.e.[b]	n.e.
3. the pyramids of the medulla oblongata	+	+	+
Supportive criteria			
Signal abnormalities in			
1. the splenium of the corpus callosum	+	+	+
2. the posterior limb of the internal capsule	+	+	+
3. the medial lemniscus in the brain stem	+	+	+
4. the superior cerebellar peduncles	+	+	+
5. the inferior cerebellar peduncles	+	n.e.	n.e.
6. the intraparenchymal part of the trigeminal nerve	−	n.e.	n.e.
7. the mesencephalic trigeminal tracts	+	n.e.	n.e.
8. the anterior spinocerebellar tracts in the medulla	+	n.e.	n.e.
9. the cerebellar white matter with subcortical preponderance	−	−	−
Elevated lactate of abnormal cerebral white matter (MRS)	+	Not performed	+

LBSL, leukoencephalopathy with brain stem and spinal cord involvement, and lactate elevation; MRI, magnetic resonance imaging; MRS, magnetic resonance spectroscopy.
[a]Homogeneous and confluent abnormal high intensity was observed, but sparing the U-fibers was unclear because of the strenuous pathological change in the white matter.
[b]n.e., not evaluated as MRI images were unavailable.

(unidentified) modifier effect in the family and (ii) this particular homozygous mutation caused the severe variant because of the substantially decreased normal protein level, although it is not full proof.

Interestingly, affected allele frequency varies, depending on the ethnicity. For example, *DARS2* mutations are the most common causes of childhood onset leukoencephalopathy in Finland, because of high carrier frequency (1:95 for the c.228-20_21delTTinsC and 1:380 for the c.492+2T>C) (4). Thus, further analysis of the *DARS2* gene in LBSL as well as childhood-to-adult onset leukoencephalopathy of unknown cause in different populations would lead us to fully understand phenotypes of the *DARS2* abnormalities.

Acknowledgements

We thank all the patients and their families for participating in this work. We also thank Ms. Y. Yamashita for her technical assistance. This work was supported by Research Grants from the Ministry of Health, Labour and Welfare (N. M., H. S., and N. M.), the Japan Science and Technology Agency (N. M.), Grant-in-Aid for Scientific Research from Japan Society for the Promotion of Science (N. M.), Grant-in-Aid for Young Scientist from Japan Society for the Promotion of Science (N. M. and H. S.), Grant for 2010 Strategic Research Promotion of Yokohama City University (N. M.), Research Grants from the Japan Epilepsy Research Foundation (H. S.), and Research Grant from Naito Foundation (N. M.), the Takeda Science Foundation (N. M. and N. M.), the Yokohama Foundation for Advancement of Medical Science (N. M.), and the Hayashi Memorial Foundation for Female Natural Scientists (N. M.).

N Miyake[a]
S Yamashita[b]
K Kurosawa[c]
S Miyatake[a]
Y Tsurusaki[a]
H Doi[a]
H Saitsu[a]
N Matsumoto[a]
[a]Department of Human Genetics, Yokohama City University Graduate School of Medicine, Yokohama, Japan,
[b]Division of Child Neurology, and
[c]Division of Medical Genetics, Kanagawa Children's Medical Center, Yokohama, Japan

References

1. van der Knaap MS, van der Voorn P, Barkhof F et al. A new leukoencephalopathy with brainstem and spinal cord involvement and high lactate. Ann Neurol 2003: 53: 252–258.
2. Scheper GC, van der Klok T, van Andel RJ et al. Mitochondrial aspartyl-tRNA synthetase deficiency causes leukoencephalopathy with brain stem and spinal cord involvement and lactate elevation. Nat Genet 2007: 39: 534–539.
3. Uluc K, Baskan O, Yildirim KA et al. Leukoencephalopathy with brain stem and spinal cord involvement and high lactate:

a genetically proven case with distinct MRI findings. J Neurol Sci 2008: 273: 118–122.
4. Isohanni P, Linnankivi T, Buzkova J et al. *DARS2* mutations in mitochondrial leucoencephalopathy and multiple sclerosis. J Med Genet 2010: 47: 66–70.
5. Lin J, Faria EC, Da Rocha AJ et al. Leukoencephalopathy with brainstem and spinal cord involvement and normal lactate: a new mutation in the *DARS2* gene. J Child Neurol 2010: 25: 1425–1428.
6. Miyake N, Kosho T, Mizumoto S et al. Loss-of-function mutations of *CHST14* in a new type of Ehlers-Danlos syndrome. Hum Mutat 2010: 31: 966–974.

Correspondence:
Noriko Miyake, MD, PhD
Department of Human Genetics
Yokohama City University Graduate School of Medicine
3-9 Fukuura
Kanazawa-ku
236-0004 Yokohama
Japan
Tel.: +81 45 787 2606
Fax: +81 45 786 5219
e-mail: nmiyake@yokohama-cu.ac.jp

SHORT REPORT

Rapid detection of a mutation causing X-linked leucoencephalopathy by exome sequencing

Yoshinori Tsurusaki,[1] Hitoshi Osaka,[2] Haruka Hamanoue,[1] Hiroko Shimbo,[2] Megumi Tsuji,[2] Hiroshi Doi,[1] Hirotomo Saitsu,[1] Naomichi Matsumoto,[1] Noriko Miyake[1]

[1]Department of Human Genetics, Yokohama City University Graduate School of Medicine, Yokohama, Japan
[2]Division of Neurology, Clinical Research Institute, Kanagawa Children's Medical Center, Yokohama, Japan

Correspondence to
Dr Noriko Miyake, Department of Human Genetics, Yokohama City University Graduate School of Medicine, 3-9 Fukuura, Kanazawa-ku, Yokohama 236-0004, Japan; nmiyake@yokohama-cu.ac.jp

Received 20 October 2010
Revised 14 December 2010
Accepted 5 February 2011
Published Online First 17 March 2011

ABSTRACT

Background Conventional PCR-based direct sequencing of candidate genes for a family with X-linked leucoencephalopathy with unknown aetiology failed to identify any causative mutations.

Objective To carry out exome sequencing of entire transcripts of the whole X chromosome to investigate a family with X linked leucoencephalopathy.

Methods and results Next-generation sequencing of all the transcripts of the X chromosome, after liquid-based genome partitioning, was performed on one of the two affected male subjects (the proband) and an unaffected male subject (his brother). A nonsense mutation in *MCT8* (c.1102A→T (p.R368X)) was identified in the proband. Subsequent PCR-based direct sequencing of other family members confirmed the presence of this mutation, hemizygous in the other affected brother and heterozygous in the proband's mother and maternal grandmother. *MCT8* mutations usually cause abnormal thyroid function in addition to neurological abnormalities, but this proband had normal thyroid function.

Conclusion Single-lane exome next-generation sequencing is sufficient to fully analyse all the transcripts of the X chromosome. This method is particularly suitable for mutation screening of X-linked recessive disorders and can avoid biases in candidate gene choice.

INTRODUCTION

High-throughput, next-generation sequencing (NGS) can have a tremendous impact on human genetic research.[1] Even personal whole-genome analysis is possible,[2] but the cost of obtaining and analysing an entire genome from many people is still unrealistic for many laboratories. Selection and enrichment of regions of interest (genome partitioning) enable us to use NGS efficiently for reasonable numbers of patients with genetic disorders.[3–6]

Ready-to-use microarray-based and solution-based hybridisation systems are now commercially available. A combination of genome partitioning using these systems and NGS is one of the most promising ways to identify genes causing Mendelian disorders.[3 4 6]

Here, we performed exome sequencing of entire transcripts of the whole X chromosome to investigate a family with X linked leucoencephalopathy with unknown aetiology after intensive candidate gene analysis by conventional exon-by-exon Sanger sequencing. A single-lane run of NGS on only two family members successfully determined the leucoencephalopathy-causing mutation.

SUBJECTS AND METHODS

A family with X-linked leucoencephalopathy

The proband (III-2) was a 13-year-old boy. He was born to Japanese consanguineous parents (II-3, 4) after an uneventful pregnancy (figure 1A). His birth weight was 3440 g. Congenital horizontal nystagmus was noted as a neonate. Because of his poor weight gain and developmental delay, he was referred to us at age 5 months. He showed progressive spasticity and dystonia with exaggerated deep tendon reflexes as well as myoclonic and tonic seizures, which responded to valproic acid and clonazepam at age 21 months. Brain MRI at 2 years showed diffuse hyperintensity of the frontal lobe on T2-weighted images, suggesting hypomyelination, and normal T1-weighted images (figure 1B,C). The peak latency intervals in auditory brainstem responses (I–V/III–V) were 4.63/2.37 ms, which were elongated compared with those of age-matched controls (4.24±0.08/1.97±0.08 ms (mean±SD)). He was clinically diagnosed with Pelizaeus–Merzbacher disease (MIM#312080), although neither mutation nor duplication was found in *PLP1* (RefSeq Gene ID, NM_000533) or *GJA12* (NM_020435) (the duplication in *GJA12* was not checked). He was never able to follow objects or control his head.

The dystonia worsened and he is now mechanically ventilated because of tracheomalacia. A thyroid function test at age 13 years indicated all normal levels: free tri-iodothyronine (T_3) 1.2 ng/ml (normal range 0.8–1.6 ng/ml), free thyroxine (T_4) 6.4 μg/dl (normal range 6.1–12.4 μg/dl) and thyroid-stimulating hormone 1.2 μIU/ml (normal range 0.5–5 μIU/ml). Brain MRI at age 13 years demonstrated improvement of myelination in the white matter, but he still presented with severe mental retardation (figure 1D,E). His younger brother was an 8-year-old boy (III-3) with an almost identical clinical course and MRI findings. His grandparents (I-1, I-2) were both healthy. The elder uncle (II-1) died at age 27 years who, initially, could walk with support but who declined towards the end of his life. Another uncle (II-2) was diagnosed with cerebral palsy and died at 7 months of age of unknown causes.

Informed consent was obtained from the patient's family members in accordance with human study protocols approved by the

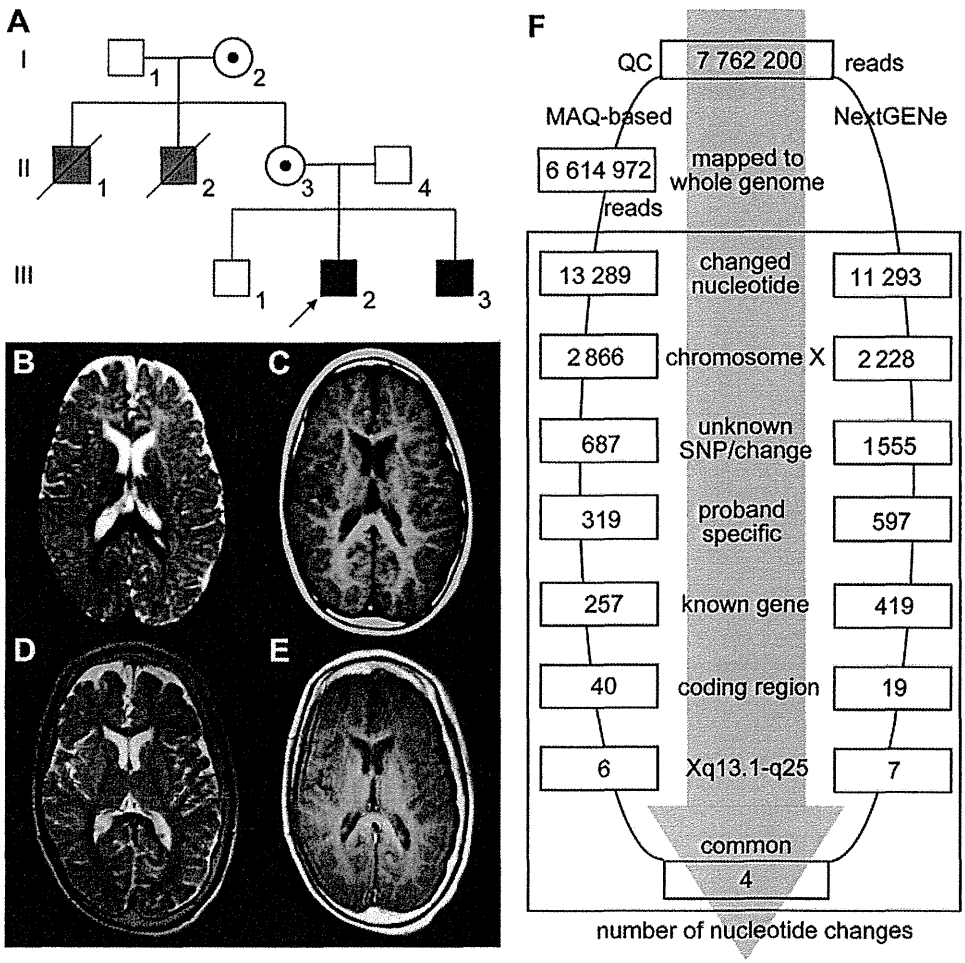

Figure 1 Pedigree and brain MRI of the proband. (A) Family pedigree. (B) T2-weighted image at age 2 years shows diffuse hyperintensity, especially in the frontal lobe. (C) T1-weighted image at 2 years shows nearly complete myelination. (D and E) At age 13 years, both T2 (D) and T1 (E)-weighted images demonstrate complete myelination; the hypomyelination observed at age 2 years can therefore be regarded as delayed myelination. (F) Flow of informatics analysis. A MAQ-based method and NextGENe analysis were performed (III-2). The selection methods included variation relative to the human genome reference sequence; variants mapped to the X chromosome; unknown variants (excluding registered SNPs); variants identified in the proband only (not in his healthy brother); variants in known genes; coding region variants; variants in genes at Xq13.1–q25; and variants common to the two informatics methods. MAQ, Mapping and Assembly with Qualities; SNP, single nucleotide polymorphism.

institutional review board at Kanagawa Children's Medical Centre and Yokohama City University School of Medicine.

Genome-wide single nucleotide polymorphism (SNP) genotyping

Genome-wide SNP genotyping was undertaken for individuals I-1, I-2, II-3, II-4, III-1, III-2 and III-3 using the GeneChip Human Mapping 10K Array *Xba* 142 2.0 (Affymetrix Inc, Santa Clara, California, USA), according to the manufacturer's protocols. Mendelian errors in the pedigree to exclude conflicted SNPs were checked using GeneChip operating software 1.2 (Affymetrix) and batch analysis in GeneChip genotyping analysis software 4.0 (Affymetrix), with the default settings for a mapping algorithm. Copy Number Analyzer for GeneChip 2.0 was used to validate copy number alterations.[7] The linked region with SNPs shared between individuals III-2 and III-3 (not observed in III-1) was checked manually.

Genome partitioning, short-read sequencing and sequence alignment

Genomic DNAs from the proband (III-2) and his unaffected brother (III-1) were used for this study. Three micrograms of DNA were processed using a SureSelect X chromosome test kit (1582 transcripts covering 3053 kb) (Agilent Technologies, Santa Clara, California, USA), according to the manufacturer's instructions. Captured DNAs were analysed using an Illumina GAIIx (Illumina Inc, San Diego, California, USA). We used only one of the eight lanes of the flow cell (Illumina), performing single 76 bp reads for each sample. Image analysis and base calling were performed by sequence control software (SCS) real-time analysis (Illumina) and/or offline Basecaller software v1.6 (Illumina) and CASAVA software v1.6 (Illumina). Reads were aligned to the human reference genome sequence (UCSC hg18, NCBI build 36.1) using the ELAND v2 program (Illumina). Coverage was calculated statistically. Identified variants were annotated based on novelty, impact on the encoded protein, the number and frequency of reads and conservation. NextGENe software v1.99 (SoftGenetics, State College, Pennsylvania, USA) was also used to analyse reads, with the default settings.

Mapping strategy and variant annotation

Approximately 9.9 million reads from III-1 (the unaffected sibling) and 7.8 million reads from III-2 (the proband), which passed the quality control (Path Filter), were mapped to the human reference genome by Mapping and Assembly with Qualities (MAQ)[8] and NextGENe software (SoftGenetics) (figure 1F). The bait region of the X chromosome based on the manufacturer's information was carefully evaluated. MAQ was able to align 7 359 688 and 6 614 972 reads to the whole genome for III-1 and III-2, respectively, which were statistically analysed for coverage using a script created by BITS Co Ltd (Tokyo, Japan). SNPs and indels were extracted from the alignment data using another script created by BITS, along with information on registered SNPs (dbSNP build 130). A consensus quality score of ≥40 was used for the SNP analysis in MAQ.

Capillary sequencing

Possible pathological variants were confirmed by Sanger sequencing using an ABI 3500xl or ABI3100 autosequencer (Life Technologies, Carlsbad, California, USA), following the manufacturer's protocol. Sequencing data were analysed by

Sequencher software (Gene Codes Corporation, Ann Arbor, Michigan, USA).

RESULTS AND DISCUSSION

Coverage analysis showed that 78.9% of all the X chromosome transcripts were completely covered by reads, and that 11.6% of transcripts were at least 90% covered. Almost all (99%) of these regions were covered by 20 reads or more (100 reads or more in 97%) by only single-lane sequencing. SNP genotyping was able to delineate the minimal linked region from rs763739 to rs1073455 (UCSC genome browser hg19 assembly, X chromosome coordinates: 76 804 990–126 844 262) (50 Mb). The maximum linked region was from rs1926354 to rs859587 (UCSC genome browser coordinates: 68 404 915–128 933 907) (60.5 Mb). Exome GAIIx sequencing with the two informatics methods identified four potentially interesting changes in the maximum linked region: c.1102AT (p.R368X) in *MCT8* (NM_006517; alternatively called *SLC16A2*); c.1402T→G (p.S468A) and c.1943A→G (p.H648R) in *CYLC1* (NM_021118); and c1606G→A (p.D536N) in *LRCH2* (NM_020871) (figure 1F). c.1102A→T (p.R368X) in *MCT8* was found heterozygously in the proband's healthy mother (II-3) and maternal grandmother (I-2), and hemizygously in the proband and his affected younger brother; each was confirmed by Sanger sequencing (figure 2). This change was not present among 92 normal female controls (0/184 alleles).

The *MCT8* gene encodes a thyroid hormone transporter and is implicated in syndromic X-linked mental retardation, Allan–Herndon–Dudley syndrome and Pelizaeus–Merzbacher-like disease (PMLD).[9–12] This nonsense mutation, c.1102A→T (p.R368X), which might lead to nonsense-mediated decay resulting in no protein production, is highly likely to be pathological. Based on the human gene mutation database (http://www.hgmd.cf.ac.uk/ac/index.php), three nonsense mutations in this gene have been previously registered: p.R245X, p.Q335X and p.S448X. The other identified variants, in *CYLC1* and *LRCH2*, are all SNPs because they were identified in normal controls: c.1402T→G (*CYLC1*): 5/182 alleles, c.1943A→G (*CYLC1*): 12/184 alleles and c1606G→A (*LRCH2*): 5/184 alleles. We concluded that the *MCT8* mutation was pathogenic in this family.

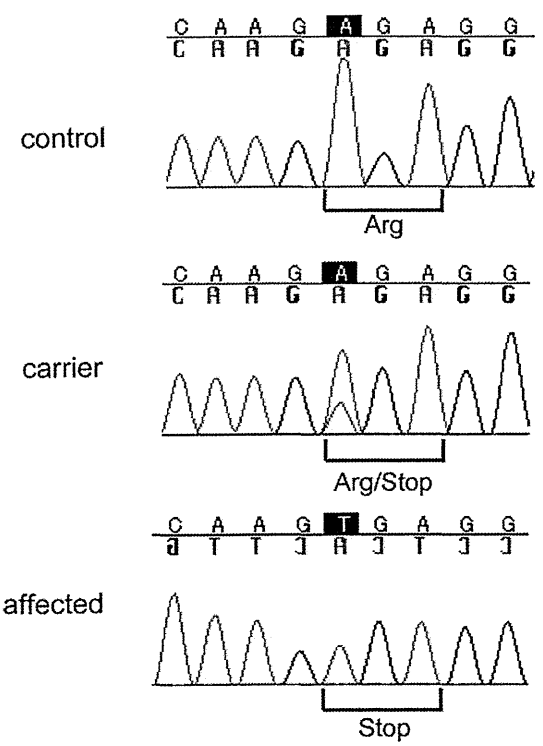

Figure 2 Electropherograms of a normal control, a carrier (mother) and the affected proband.

PMLD caused by *MCT8* mutations presents with infantile hypotonia, severe psychomotor development, nystagmus, generalised muscle weakness, dystopia, joint contracture and progressive spastic paraplegia. All affected male subjects develop the disease, while heterozygous female subjects are clinically normal or sometimes show mild thyroid dysfunction.[9 12] Brain MRI shows delayed myelination in the first few years of life, which subsequently improves but with residual neurological disability. The unique diagnostic feature of the disease is an abnormal thyroid hormone profile: increased free T_3, decreased free T_4 and normal thyroid-stimulating hormone.[12] The cases we analysed here showed clinical features and brain MRI findings typical of PMLD, but no thyroid hormone abnormalities. Based on regular laboratory testing and conventional PCR-based gene screening, we might have failed, or taken much longer, to identify the causative mutation. Thus, unbiased screening without prior knowledge is one of the advantages of NGS.

Thyroid hormone (T_4 and T_3) is important in neuronal development and its deficiency in the pre/neonatal stage causes a form of mental retardation called cretinism. T_4 is released from the thyroid as a prohormone and is altered to biologically active T_3 by iodothyronine deiodinases.[13] Active T_3 is delivered to the peripheral organs via thyroid hormone transporters. MCT8 is a thyroid hormone-specific transporter and is mainly expressed in the brain and liver.[14 15] In MCT8 deficiency, T_3 and T_4 uptake is impaired and deiodinase 2 is activated.[16] This results in increased serum T_3 levels because of T_3 accumulation in the peripheral blood. In previous reports, the majority of patients showed abnormal levels of thyroid hormones, but some displayed values within the normal range.[9 10 12 17 18] The variable range for abnormal thyroid hormone levels might be explained by unidentified modifier effect(s) and/or other transporter(s) that can compensate for MCT8 function.[19] Additionally, although MCT8 deficiency has been determined by abnormalities in thyroid function tests, it is unknown what proportion of the patients with MCT8 deficiency show abnormal thyroid function. We suggest that it is important to evaluate thyroid hormone function in PMLD with unknown cause.

Before the exome NGS analysis, we screened *PLP1*, *GJA12*, and seven other candidate genes mapped to the linked region: *MSN* (NM_002444), *IGBP1* (NM_001551), *SNX12* (NM_013346), *OGT* (NM_181672), *HDAC8* (NM_018486), *SH3BGRL* (NM_003022.2) and *PCDH11X* (NM_032967.2). Because we found no pathological changes, we adopted the exome sequencing strategy. We determined that exome sequencing with a single lane for each sample was sufficient to analyse all the transcripts of the X chromosome. In X-linked recessive diseases, male subjects are usually affected, and therefore the single X chromosome is the primary target of exome sequencing. Except for mosaic mutations, the hemizygous (rather than heterozygous) status of disease-related nucleotide changes is relatively easy to detect using all-or-none NGS reads (0% or 100% of reads). There was no difference in the ability of our two informatics methods (MAQ and NextGENe) to detect pathological changes. This approach could equally be applied to the analysis